Pergamon

Tetrahedron Letters, Vol. 37, No. 46, pp. 8409-8412, 1996

0040-4039/96 $15.00 + 0.00

PII: S0040-4039(96)01923-5

Synthesis and Characterization of Intra- and Intermolecular Hydrogen Bonding Isomers of P–H (apical) Phosphoranes Bearing a Hydroxyl Group and Their Thermal Cyclization

Kazumasa Kajiyama,† Satoshi Kojima and Kin-ya Akiba*

Department of Chemistry, Faculty of Science, Hiroshima University,
1-3-1 Kagamiyama, Higashi-Hiroshima 739, Japan

Abstract: The reaction of spirophosphorane **1** with 3 equivalents of RLi (R = Me, *n*-Bu, *t*-Bu) in Et_2O at –78 °C followed by treatment with aq. HCl gave monocyclic P–H phosphoranes **2**–**4** bearing an apical hydrogen atom in good yields. Particularly in the case of **4**, an isomer **4a** with intramolecular hydrogen bonding and an isomer **4b** with intermolecular hydrogen bonding with a solvent molecule could be separately isolated. Monocyclic phosphoranes **2**–**4** cyclized intramolecularly with elimination of H_2 to form spirophosphoranes **5**–**7** upon heating. Kinetic examination of cyclizations implied that they proceed via four-membered ring transition states involving hexacoordinate phosphorus.

The heterolysis of element-carbon or element-hydrogen bonds which gives compounds bearing new element-heteroatom bonds with elimination of hydrocarbon or H_2 has been implicated to involve species of higher coordination number during the reaction.[1] As part of our continuous studies on hypervalent organic compounds, we have found that in the intramolecular cyclization reaction of a series of acyclic 8-Si-4[2] *o*-silylbenzyl alcohols (weak acids) to 8-Si-4 cyclic alkoxysilanes, the selectivity of the eliminating hydrocarbon is highly dependent on the relative stabilities of isomeric 10-Si-5 transition states.[3] This showed the importance of participation of the hypervalent bond in the transition state besides acidity of the eliminating hydrocarbons.[4] In analogous transformation of monocyclic 10-Bi-5 alcohols to bicyclic 10-Bi-5 bismuthanes the intermediacy of hexacoordinate 12-Bi-6 species could be verified.[5] Herein we report on the synthesis of monocyclic P–H (apical) phosphoranes (10-P-5) which bear a hydroxyl group and thermal cyclization reactions to give 10-P-5 spirophosphoranes with elimination of H_2.

The phosphoranes **2**–**4** were prepared by the reaction of P–H (equatorial) spirophosphorane **1** with 3 equivalents of alkyl lithium reagents in Et_2O at –78 °C followed by careful treatment with aq. HCl (Scheme 1): **2** [y. 68 %, δ_P ($CDCl_3$) = –51.9, $^1J_{P\text{-}H}$ = 276 Hz], **3** [y. 90 %, δ_P ($CDCl_3$) = –34.4, $^1J_{P\text{-}H}$ = 273 Hz], and a mixture of **4a** [δ_P ($CDCl_3$) = –14.7, $^1J_{P\text{-}H}$ = 273 Hz] and **4b** [δ_P ($CDCl_3$) = –42.7, $^1J_{P\text{-}H}$ = 293 Hz] (combined y. 92 %).[6] The reaction involves the nucleophilic reaction of RLi to the 10-P-4 phosphoranide generated by incipient deprotonation of **1** to give a ring opened dianionic species, which is diprotonated upon acidic workup. Isomers **4a** and **4b** could each be crystallized out as single compounds by changing the solvent, nondonor solvents (cyclohexane-CCl_4) for the former and donor solvents (CH_3CN or EtOH) for the latter. Cyclized products, 10-P-5 spirophosphoranes **5** (R = Me) and **6** (R = *n*-Bu), were obtained as minor products in 22% and 9% yields, respectively, whereas no P–*t*-Bu spirophosphorane **7** was obtained in the case of **4**.[7] In the case of phosphorane **2** (R = Me) partial cyclization was found to occur even on PTLC (hexane–CH_2Cl_2 = 5 : 1), while partial cyclization was observed during recrystallization of **2** and **3** from hexane–CH_2Cl_2. These results indicate that the order of stability of monocyclic phosphoranes towards cyclization is **2** < **3** < **4**. Although intermediates could not be isolated, similar alkyl and aryl spirostiboranes have been obtained in nucleophilic reactions to a 10-Sb-4 stiboranide.[8]

Scheme 1

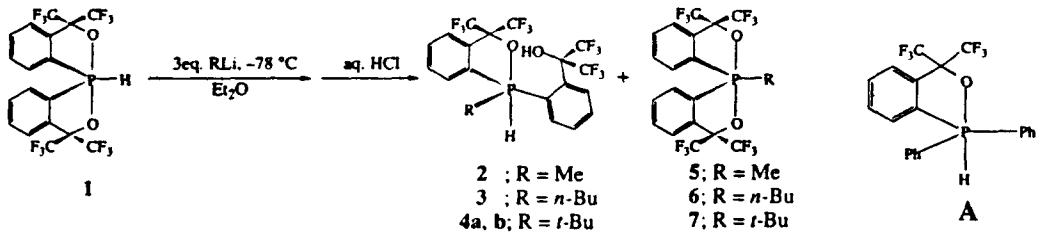

The $^{1}J_{P-H}$ coupling constants (273–293 Hz) of monocyclic phosphoranes **2**–**4** revealed the presence of an apical hydrogen in solution and are in good agreement with the reported value of 266 Hz for a similar compound **A** ($CDCl_3$, δ_P = –49.3).[9] In contrast, $^{1}J_{P-H}$ coupling constant of spirophosphorane **1** ($CDCl_3$, δ_P = –45.8) bearing an equatorial hydrogen was 729 Hz.[10] X-ray structural analysis of monocyclic phosphoranes **2**, **3**, **4a**, and **4b** were carried out, of which **4a** (R = *t*-Bu, Figure 1)[11] and **4b** (R = *t*-Bu, Figure 2)[12] are shown. The structures of **2** and **3** were essentially the same as **4a**, differing only in the alkyl substituent. Compounds **4a** and **4b** were found to differ only in the hydrogen bonding partner of the hydroxyl group, the former intramolecularly with the apical oxygen of the bidentate and the latter intermolecularly with the nitrogen atom of CH_3CN, a solvent molecule. This is the first structural characterization of hydrogen bonding isomers involving hypervalent phosphorus. The P–O (apical) bond is longer in **4a** [1.922(5)] than in **4b** [1.865(2)]. This could be considered a consequence of weakening of this polarizable bond by the intramolecular hydrogen bonding.

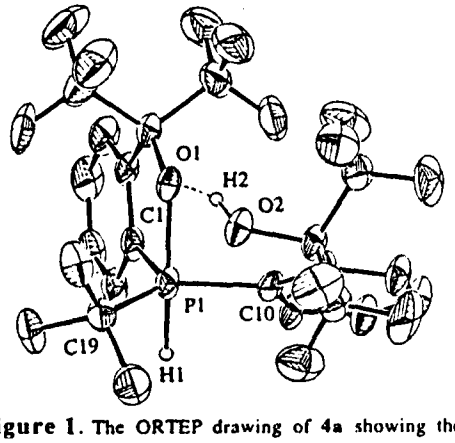

Figure 1. The ORTEP drawing of **4a** showing the thermal ellipsoids at the 30 % probability level. All the hydrogens besides (P1–)H1 and (O2–)H2 have been ommitted for clarity. Selected bond distances (Å) and angles (deg): **P1–O1, 1.922(5)**; P1–H1, 1.47(7); P1–C1, 1.790(7); P1–C10, 1.881(7); P1–C19, 1.854(9); **O2–H2, 1.2(2)**; **O1–H2, 1.4(1)**; **P1–O2, 3.131**; O1–P1–H1, 172(3); O1–P1–C1, 83.6(3); C1–P–C10, 111.4(3); C1–P–C19, 119.5(4); C10–P-C19, 129.1(4).

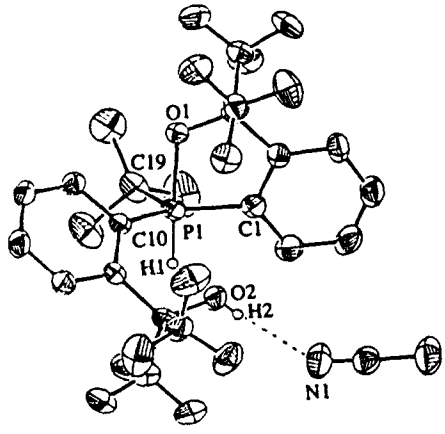

Figure 2. The ORTEP drawing of **4b**·CH_3CN showing the thermal ellipsoids at the 30 % probability level. All the hydrogens besides (P1–)H1 and (O2–)H2 have been ommitted for clarity. Selected bond distances (Å) and angles (deg): **P1–O1, 1.865(2)**; P1–H1, 1.33(3); P1–C1, 1.826(2); P1–C10, 1.855(2); P1–C19, 1.878(3); **O2–H2, 0.66(4)**; **N1–H2, 2.16(4)**; **P1–O2, 2.84**; O1–P1–H1, 175(1); O1–P1–C1, 84.1(1); C1–P–C10, 131.2(1); C1–P–C19, 117.0(1); C10–P-C19, 111.5(1).

Kinetic examination of the thermal cyclization of **2**–**4** to spirophosphoranes **5**–**7**, respectively, was next carried out (Scheme 2). The cyclization of **2** to **5** was too fast to monitor. The rates of cyclization of **3** to **6** were measured in toluene-d_8 (343–373 K) and *o*-dichlorobenzene (343–373 K) by monitoring ^{19}F

NMR. In the case of cyclization of **4** to **7**, the rates in *p*-xylene (393–423 K) and *o*-dichlorobenzene (393–423 K) were measured by monitoring ^{31}P NMR because of the complexness of the ^{19}F NMR spectra. In *o*-dichlorobenzene, spirophosphorane **1** [38 % (423 K)] was also formed with **7** [62 % (423 K)]. All the process followed first-order kinetics quite satisfactorily until a half life. The Eyring plot of the rates also turned out to be linear thus implying the existence of only a single process for the cyclization. Representative rates and activation parameters are shown in Table 1.

Scheme 2

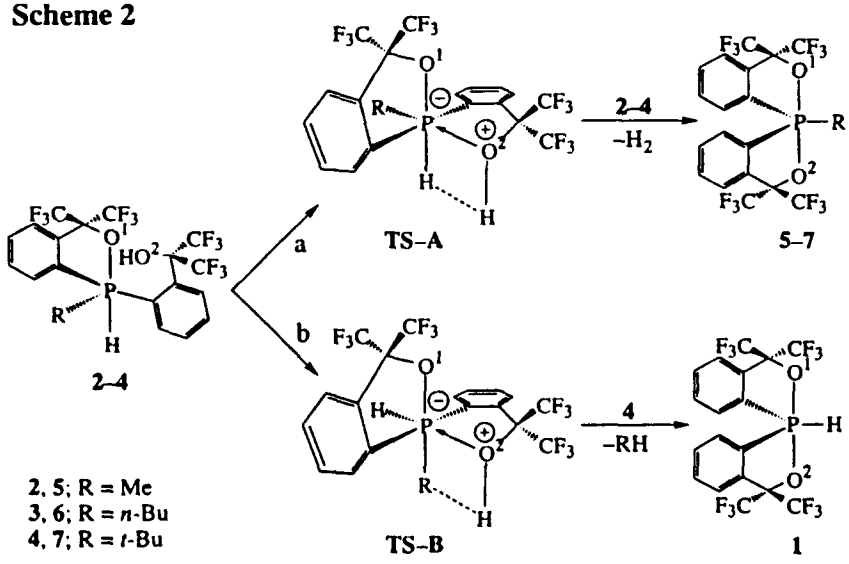

Table 1. Kinetic Parameters of the Cyclization of Phosphoranes **3** and **4**

phosphorane	solvent	product	k <sec^{-1}> (T <K>)	$\Delta G^{\ddagger}$ <kcal mol^{-1}> (T <K>)	$\Delta H^{\ddagger}$ <kcal mol^{-1}>	$\Delta S^{\ddagger}$ <eu>
3	toluene-d_8	6	(1.46 ± 0.03) x 10^{-5} (373)	30.3 (373)	17.3 ± 0.6	−34.7 ± 1.7
	o-dichlorobenzene	6	(5.55 ± 0.05) x 10^{-5} (373)	29.3 (373)	14.0 ± 0.2	−41.0 ± 0.6
4	*p*-xylene	7	(2.30 ± 0.04) x 10^{-5} (423)	34.0 (423)	32.2 ± 1.1	−4.2 ± 2.6
	o-dichlorobenzene	7	(3.22 ± 0.07) x 10^{-5} (423)	33.7 (423)	29.5 ± 0.7	−9.9 ± 1.8
		1	(1.92 ± 0.03) x 10^{-5} (423)	34.2 (423)	25.0 ± 1.0	−21.8 ± 2.6

The cyclization rates of phosphoranes **3** and **4** in more polar *o*-dichlorobenzene (E_T^N = 0.225) were faster than those in nonpolar toluene-d_8 (E_T^N = 0.099) and *p*-xylene (E_T^N = 0.074). The difference in the activation enthalpies in both solvents were ca. 3 kcal mol^{-1} for both compounds, while the difference between **3** and **4** was ca. 15 kcal/mol. The activation entropies of **3** were large negative values and those of **4** were negative but the magnitude was much smaller. These results suggest that the intramolecular cyclization reactions of phosphoranes **2**–**4** with elimination of H_2 proceed via a polarized, concerted four-membered transition state with the involvement of hexacoordinate phosphorus species which is considerably more congested than the pentacoordinate ground state as depicted in Scheme 2. In the case of **4** to **7**, the ground state is probably already highly motionally hindered due to the back strain of the *t*-Bu group. That the magnitude of the activation entropy of the formation of **1** is larger than that of **7** is probably because the *t*-butyl group itself participates in the bond transformation in the transition state (**TS-B**). The large difference in activation enthalpy between **3** and **4** probably reflects the reluctance for **4** to cyclize due to much larger steric hindrance.

References and Notes

†. Research Fellow of the Japan Society for the Promotion of Science.

1. For example: Abraham, M. H.; Grellier, P. L. In *The Chemistry of the Metal-Carbon Bond*; Hartley F.; Patai, S., Eds. John Wiley and Sons: New York, 1985; Vol. 2, Chapter 2.

2. For designation: Perkins, C. W.; Martin, J. C.; Arduengo, A. J.; Lau, W.; Alegria, A.; Kochi, J. K. *J. Am. Chem. Soc.* **1980**, *102*, 7753-7759.

3. Yamamoto, Y.; Takeda, Y.; Akiba, K.-y. *Tetrahedron Lett.* **1989**, *30*, 725-728 and unpublished results.

4. (a) Depuy, C. H.; Bierbaum, L. W.; Damrauer, R. *J. Am. Chem. Soc.* **1984**, *106* 4051-4053. (b) Davis, L. P.; Burggraf, L. W.; Gordon, M. S. *J. Am. Chem. Soc.* **1988**, *110*, 3056-3062.

5. Yamamoto, Y.; Ohdoi, K.; Chen, X.; Kitano, M.; Akiba, K.-y. *Organometallics* **1993**, *12*, 3297-3303.

6. Elemental analyses of all compounds are within 0.4 % of calculated values. **2**: m.p. 101 °C; ^{1}H NMR ($CDCl_3$) δ 8.86 (br s, 1H), 8.10–7.90 (m, 1H), 7.79 (br s, 4H), 7.55–7.20 (m, 3H), 6.37 (dq, $^1J_{H\text{-}P}$ = 276 Hz, $^3J_{H\text{-}H}$ = 3.9 Hz, 1H), 2.44 (dd, $^2J_{H\text{-}P}$ = 14.7 Hz, $^3J_{H\text{-}H}$ = 3.9 Hz, 3H); ^{19}F NMR ($CDCl_3$) δ -72.9 (br s, 3F), -76.3 (br s, 3F), -76.9 (br s, 3F), -77.0 (br s, 3F); ^{31}P NMR ($CDCl_3$) δ -51.9. **3**: m.p. 119 °C; ^{1}H NMR ($CDCl_3$) δ 9.13 (br s, 1H), 8.07–8.02 (m, 1H), 7.89–7.85 (m, 1H), 7.80–7.72 (m, 3H), 7.55–7.48 (m, 1H), 7.45–7.41 (m, 1H), 7.36–7.32 (m, 1H), 6.16 (dd, $^1J_{H\text{-}P}$ = 273 Hz, $^3J_{H\text{-}H}$ = 5.9 Hz, 1H), 3.21–3.06 (m, 1H), 2.69–2.52 (m, 1H), 1.65–1.46 (m, 1H), 1.45–1.36 (m, 2H), 1.35–1.22 (m, 1H), 0.88 (t, $^3J_{H\text{-}H}$ = 7.3 Hz, 3H); ^{19}F NMR ($CDCl_3$) δ -72.9 (br s, 3F), -76.3 (q, $^4J_{F\text{-}F}$ = 9.2 Hz, 3F), -76.8 (q, $^4J_{F\text{-}F}$ = 8.2 Hz, 3F), -77.0 (qq, $^4J_{F\text{-}F}$ = 9.2 Hz, $^9J_{F\text{-}F}$ = 4.9 Hz, 3F); ^{31}P NMR ($CDCl_3$) δ -34.4. **4a**: m.p. 108 °C; ^{1}H NMR ($CDCl_3$) δ 8.58 (br s, 1H), 8.00–7.89 (m, 1H), 7.80–7.48 (m, 7H), 5.81 (d, $^1J_{H\text{-}P}$ = 273 Hz, 1H), 1.30 (d, $^3J_{H\text{-}P}$ = 23.4 Hz, 9H); ^{19}F NMR ($CDCl_3$) δ -73.4 (q, $^4J_{F\text{-}F}$ = 9.5 Hz, 3F), -73.5 (q, $^4J_{F\text{-}F}$ = 9.5 Hz, 3F), -74.6 (q, $^4J_{F\text{-}F}$ = 9.1 Hz, 3F), -76.1 (q, $^4J_{F\text{-}F}$ = 10.7 Hz, 3F); ^{31}P NMR ($CDCl_3$) δ -14.7. **4b***: m.p. 83–84 °C (containing EtOH); ^{1}H NMR (acetone-d_6) δ 8.77–8.72 (m, 1H), 7.87–7.82 (m, 1H), 7.75–7.63 (m, 4H), 7.63–7.54 (m, 2H), 7.48 (s, 1H), 6.07 (d, $^1J_{H\text{-}P}$ = 293 Hz, 1H), 1.17 (d, $^3J_{H\text{-}P}$ = 19.5 Hz, 9H); ^{19}F NMR (acetone-d_6) δ -73.3 (qq, $^4J_{F\text{-}F}$ = 8.9 Hz, $^9J_{F\text{-}F}$ = 3.1 Hz, 3F), -73.6 (q, $^4J_{F\text{-}F}$ = 9.5 Hz, 3F), -74.3 (q, $^4J_{F\text{-}F}$ = 8.6 Hz, 3F), -75.5 (qq, $^4J_{F\text{-}F}$ = 9.2 Hz, $^9J_{F\text{-}F}$ = 2.8 Hz, 3F); ^{31}P NMR (acetone-d_6) δ -40.1. (*: NMR data was taken after removal of EtOH.)

7. Elemental analyses of all compounds are within 0.4 % of calculated values. **5**: m.p. 134 °C; ^{1}H NMR ($CDCl_3$) δ 8.43–8.38 (m, 2H), 7.79–7.69 (m, 6H), 2.11 (d, $^2J_{H\text{-}P}$ = 16.6 Hz, 3H); ^{19}F NMR ($CDCl_3$) δ -75.1 (q, $^4J_{F\text{-}F}$ = 9.5 Hz, 6F), -75.4 (q, $^4J_{F\text{-}F}$ = 9.5 Hz, 6F); ^{31}P NMR ($CDCl_3$) δ -22.6. **6**: m.p. 109 °C; ^{1}H NMR ($CDCl_3$) δ 8.43–8.38 (m, 2H), 7.72–7.58 (m, 6H), 2.34 (ddt, $^2J_{H\text{-}P}$ = 28.3 Hz, $^2J_{H\text{-}H}$ = 12.2 Hz, $^3J_{H\text{-}H}$ = 4.9 Hz, 1H), 2.20 (ddt, $^2J_{H\text{-}P}$ = 12.2 Hz, $^2J_{H\text{-}H}$ = 12.2 Hz, $^3J_{H\text{-}H}$ = 4.4 Hz, 1H), 1.86–1.70 (m, 1H), 1.32–1.20 (m, 3H), 0.81 (t, $^3J_{H\text{-}H}$ = 7.3 Hz, 3H); ^{19}F NMR ($CDCl_3$) δ -75.1 (q, $^4J_{F\text{-}F}$ = 9.3 Hz, 6F), -75.4 (q, $^4J_{F\text{-}F}$ = 9.3 Hz, 6F); ^{31}P NMR ($CDCl_3$) δ -18.8. **7**: m.p. 128 °C; ^{1}H NMR ($CDCl_3$) δ 8.42–8.38 (m, 2H), 7.66–7.64 (m, 6H), 1.13 (d, $^3J_{H\text{-}P}$ = 20.0 Hz, 9H); ^{19}F NMR ($CDCl_3$) δ -72.4 (q, $^4J_{F\text{-}F}$ = 10.1 Hz, 6F), -74.5 (q, $^4J_{F\text{-}F}$ = 10.1 Hz, 6F); ^{31}P NMR ($CDCl_3$) δ -9.8.

8. Akiba, K.-y.; Nakata, H.; Yamamoto, Y.; Kojima, S. *Chem. Lett.* **1992**, 1559-1562.

9. Ross, M. R.; Martin, J. C. *J. Am. Chem. Soc.* **1981**, *103*, 1234-1235.

10. (a) Granoth, I.; Martin, J. C. *J. Am. Chem. Soc.* **1979**, *101*, 4623-4626. (b) Kojima, S.; Kajiyama, K.; Akiba, K.-y. *Tetrahedron Lett.* **1994**, *35*, 7037-7040. (c) Kojima, S.; Kajiyama, K.; Akiba, K-y. *Bull. Chem. Soc. Jpn.* **1995**, *68*, 1785-1797.

11. Prisms were obtained by recrystallization from CCl_4-cyclohexane. Crystal data for **4a**: $C_{22}H_{19}F_{12}O_2P$, orthorhombic, $P2_12_12_1$, colorless, a = 14.027(4) Å, b = 16.421(4) Å, c = 10.074(3) Å, V = 2465(1) Å^3, Z = 4, R = 0.068, Rw = 0.082, GOF = 2.72. The hydroxyl hydrogen atom was located from a difference Fourier map calculated at the final stage of structure analysis.

12. Prisms were obtained by recrystallization from CH_3CN. Crystal data for **4b**·CH_3CN: $C_{24}H_{22}F_{12}NO_2P$, monoclinic, $P2_1/n$, colorless, a = 15.748(1) Å, b = 16.986(2) Å, c = 11.016(2) Å, β = 110.257(9)°, V = 2764.4(5) Å^3, Z = 4, R = 0.042, Rw = 0.068, GOF = 3.16. The hydroxyl hydrogen atom was located from a difference Fourier map calculated at the final stage of structure analysis.

(*Received in Japan* 19 *August* 1996; *revised* 24 *September* 1996; *accepted* 25 *September* 1996)